

Unsupervised Definition of the Tibia-Femoral Joint Regions of the Human Knee and its Applications to Cartilage Analysis

José Gerardo Tamez-Peña^{*}, Monica Barbu-McInnis, and Saara Totterman
VirtualScopics, Inc, 350 Linden Oaks, Rochester, NY 14625

ABSTRACT

Abnormal MR findings including cartilage defects, cartilage denuded areas, osteophytes, and bone marrow edema (BME) are used in staging and evaluating the degree of osteoarthritis (OA) in the knee. The locations of the abnormal findings have been correlated to the degree of pain and stiffness of the joint in the same location. The definition of the anatomic region in MR images is not always an objective task, due to the lack of clear anatomical features. This uncertainty causes variance in the location of the abnormality between readers and time points. Therefore, it is important to have a reproducible system to define the anatomic regions. This work presents a computerized approach to define the different anatomic knee regions. The approach is based on an algorithm that uses unique features of the femur and its spatial relation in the extended knee. The femur features are found from three dimensional segmentation maps of the knee. From the segmentation maps, the algorithm automatically divides the femur cartilage into five anatomic regions: trochlea, medial weight bearing area, lateral weight bearing area, posterior medial femoral condyle, and posterior lateral femoral condyle. Furthermore, the algorithm automatically labels the medial and lateral tibia cartilage. The unsupervised definition of the knee regions allows a reproducible way to evaluate regional OA changes. This work will present the application of this automated algorithm for the regional analysis of the cartilage tissue.

Keywords: Segmentation, Shape Analysis, Magnetic Resonance, OA, Cartilage

1. INTRODUCTION

OA has been defined by the American College of Rheumatology (ACR) as a “heterogeneous group of conditions that leads to joint symptoms and signs which are associated with defective integrity of articular cartilage, in addition to related changes in the underlying bone at the joint margins”. OA is a very debilitating disease and it has been reported that 70% of women and 60% of men aged 65 years or older suffer from osteoarthritis (OA)^{1,2}. The location of the initial condition and the components that are mainly affected are not fully studied and understood^{3,4,5,6}. Currently non-invasive technology required for the direct observation of the degenerative changes is under development^{7,8,9,10,11,17}.

The recent advances in quantitative image analysis technology of MR imaging have recently started to generate a great wealth of information on articular cartilage and bone physiology^{6,12,13,14,15,16,18,33,34}; a fair amount of work is still needed to understand all this information. Furthermore, MRI could help to identify promising drug targets and clinical therapies via monitoring structural and molecular effects of the therapy on OA; so far there is a lack of enough studies to validate MRI as an alternative endpoint to the current clinical evaluation. To help in the development of the new technologies the National Institute of Health (NIH), the National Institute of Arthritis and Musculoskeletal and Skin Diseases (NIAMS) and the pharmaceutical industry created the Osteoarthritis Initiative (OAI). The OAI is targeted at identifying the most promising OA biomarkers (including imaging) to reflect the development and progression of symptomatic knee osteoarthritis. The study involves a cohort of 5000 participants at 4 sites, all of which receive MRI of both knees at 1 year intervals for 5 years.

The interpretation of the MRI data of OA subjects will require the development of accurate and highly reproducible analysis techniques. Although a great effort has been put forward in the validation of MRI as an effective tool for the measurement of cartilage morphology^{15,17,19,20,21,22,24,26,27,28,29,30,31,35}, the sensitivity of average indexes for cartilage morphology to monitor OA progression is still not clear. We hypothesize that OA changes are highly focal; therefore global metrics are not sensitive enough to monitor changes. On the other hand, radiologists and rheumatologists have

^{*} tamez@virtualscopics.com; phone 1 585 249-6231; fax 1 585 218-7350

long recognized the value of focal evaluation of OA. They have developed scoring systems that evaluate the changes and findings according to the anatomic location^{4,11,16}. So far it has been recognized that the best evaluation of Osteoarthritis (OA) from MRI data requires objective location of cartilage defects, bone marrow edemas (BME), and other abnormal findings^{4,5,9,12,16,25,26,32}. The accurate location of the OA findings is very important for the accurate registration of results and reads among radiologist and time points. The determination of these locations is not always a simple task on the tibia-femoral joint. The boundary definition among the different anatomical locations has not been clearly defined among researchers especially for the definition of the so called weight bearing regions of the joint. The weight bearing regions are not defined by any clear landmark, making them vary from user to user and from time point to time point.

The purpose of this article is to present a highly reproducible computerized approach to define the anatomic knee regions. The method divides the cartilage in such a way that the morphological parameters for patella-femoral cartilage and tibia-femoral cartilage regions can be reported without the need of human intervention. The approach is based on the 3D joint space algorithm which has been successfully used for the analysis of the joint space³⁷. This algorithm has been extended from its initial conception to enable labeling of five unique femur cartilage regions: trochlea, medial weight bearing, lateral weight bearing, posterior medial femoral condyle, and posterior lateral femoral condyle. Then, the algorithm automatically labels the medial and lateral tibia cartilage. The unsupervised definition of the knee regions provides a reproducible way to subdivide the knee.

2. MATERIAL & METHODS

2.1. Data Sets

One knee of nine volunteers (4 male and 5 female from 31 to 71 year old and a mean age of 44), was scanned using a GE Sigma 1.5T scanner (GE, Milwaukee, WI). All volunteers consented to the study protocol which was previously approved by the Institutional Research Subjects Review Board. Two sets of images were acquired for each knee: first a sagittal 3D SPGR fat saturated sequence with a TR of 39, TE of 7.0ms, Nex 1, Flip angle of 20°, and a 256 by 256 matrix with a 14.0 cm field of view. Then a sagittal 3D GRE image with a TR of 29, TE of 15.0 sec, Nex 1, Flip angle of 40°, and a 256 by 256 matrix with a 14.0 cm field of view were acquired.

2.2. Analysis Methods

2.2.1. Image Analysis and Cartilage Extraction

The 3D SPGR and the 3D GRE scans were registered and fused. The registered and fused images were then mirrored in the coronal plane to mimic the contra-lateral knee. All mirrored and original registered and fused images were then randomized. The MRI data sets were then segmented using the approach described by Tamez-Peña^{35,36}. The segmentation starts with a hybrid segmentation algorithm, which is used to segment the rigid structures within the randomized registered and fused data sets. An expert observer used the segmented maps to label the tibia and the femur in each of the 18 randomized segmentation maps. The completed bone map and the original segmentation map were used by a cartilage extraction algorithm to identify the femur and tibia cartilage regions. The mapping of the cartilage regions is described in the next section.

2.2.2. Joint Regions Definitions

The definition of the cartilage regions follows the 3D joint space analysis delineated by Tamez-Peña³⁷. We modified and enhanced the joint space algorithm to allow labeling the femoral and tibial regions into their different components. The original joint space algorithm had the following characteristics:

- The internal-external rotation is automatically measured. The regions definitions are independent of the internal rotation of the knee.
- The width of the medial and lateral joint space compartments is automatically measured.

To apply the joint space algorithm for the division of the cartilage regions the algorithm needed to be enhanced to:

- Use of femur asymmetry to automatically identify the medial and lateral compartments of the knee. Therefore, there is no need for the user to identify the medial compartments or the fibula.
- Identify the femoral notch extension, which allows accurate estimation of the trochlea region.
- Measure the flexion of the knee, which makes definition of the weight bearing regions more robust to changes in the flexion angle.

Once we incorporated the two new requirements the full analysis of the knee regions is as follows. Using the segmentation of the femur, the algorithm starts by identifying the most distal points of the femur (Figure 1). Once those points are identified, we locate the most posterior points of the femoral condyles. Using those points the internal-external rotation of the femur is identified. The line which connects posterior points is projected to the axial plane and is used to estimate the internal-external rotation. This estimation is adjusted to the projected orientation of the most distal points of the femur. The actual correction is just 5% of the total orientation found by the most posterior points. Then the most distal points of the condyles are used to estimate the angle of the femur (varus-valgus) by projecting the points into the coronal plane. The internal-external rotation, the angle and the center are used to establish a new femur coordinate system, its center located at the centroid of the distal points of the condyles. Once the femur center coordinate system is found the next step is the identification of the width of the femoral notch. The notch width is estimated by a weighed estimation of the condyles' widths. The condyles' widths are estimated by scanning the femur segmentation from the most posterior points towards the trochlea and computing the distance between condyles' points. The steps just described are very similar to the ones used by the original joint-space algorithm³⁷. The identification of the medial and lateral side of the knee is done by scanning the most anterior point to the left of the axis and the most anterior point to the right of the trochlea. The scanning is done at each slice of the image moving seven millimeters from the most distal point of the femur and moving 35 mm up. The location of the trochlea region is done by finding the most anterior point of the intercondylar region. The most anterior point is used to define the transition between the condyles and the trochlea regions. The determination whether the knee is left or right knee is done by accumulating the points that are closest to the anterior-posterior axis. If the accumulation of points to the right is less than those points to the left, then the knee is a left knee, otherwise is a right knee. The degree of flexion is found by searching all the most posterior points of the femur shaft that are inside the MRI field of view. All those points are then fitted to a line. The angle made by the line is the one that defines the flexion angle.

Once the flexion angle is found; the femur reference frame is rotated to reflect this angle. Once the reference frame is rotated this rotated system is the new femur reference frame. At this time we have the femur reference frame and the most anterior point. The condyles are subdivided into weight bearing regions and posterior regions. The weight bearing regions are found with the aid of the tibia. Segmentation of the tibia is used to estimate the length of the weight bearing region. The length is found by searching the most anterior point of the tibial plateau and the most posterior point of the tibial plateau that are in line with the location of the most distal points of the femoral condyles. The anterior point of the medial tibia condyle and the posterior points are then projected up to the femur. The projection follows an angle to meet the femoral condyle as seen in figure 1d. The definition of the femur orientation, the intercondyle area, and the weight bearing regions are all that is needed to divide the femoral and tibia cartilage tissue into all the relevant regions: Trochlea, weight bearing aspect of the medial condyle, weight bearing aspect of the lateral condyle, posterior aspect of the medial condyle, posterior aspect of the lateral condyle, tibia medial plateau and tibia lateral plateau. These cartilage divisions are done by classifying the cartilage voxels into the different regions just by following the joint regions as seen in figure 2. Figure 3 shows a 3D reconstruction of the cartilage and bones after the extraction of the different cartilage regions.

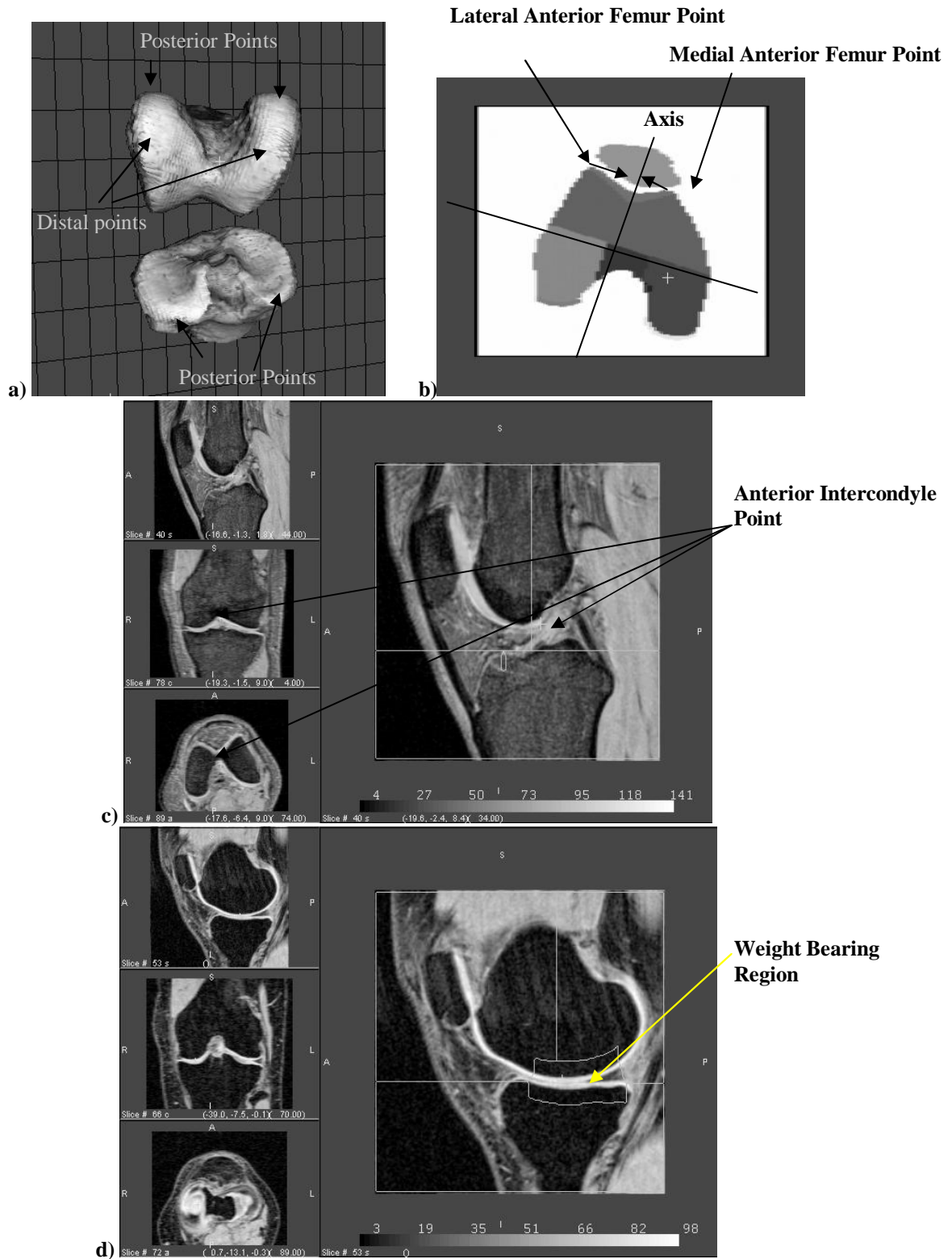


Figure 1: a) The definition of the cartilage regions starts by finding selected anatomic points of the femur. b) The orientation and the medial, lateral classification of the cartilage is done by finding the orientation and the natural asymmetry of the femur. c) The most anterior point of the intercondylar region is used to mark the definition of the trochlea and the condyles. d) The points of the tibia help in the definition of the weight bearing regions.

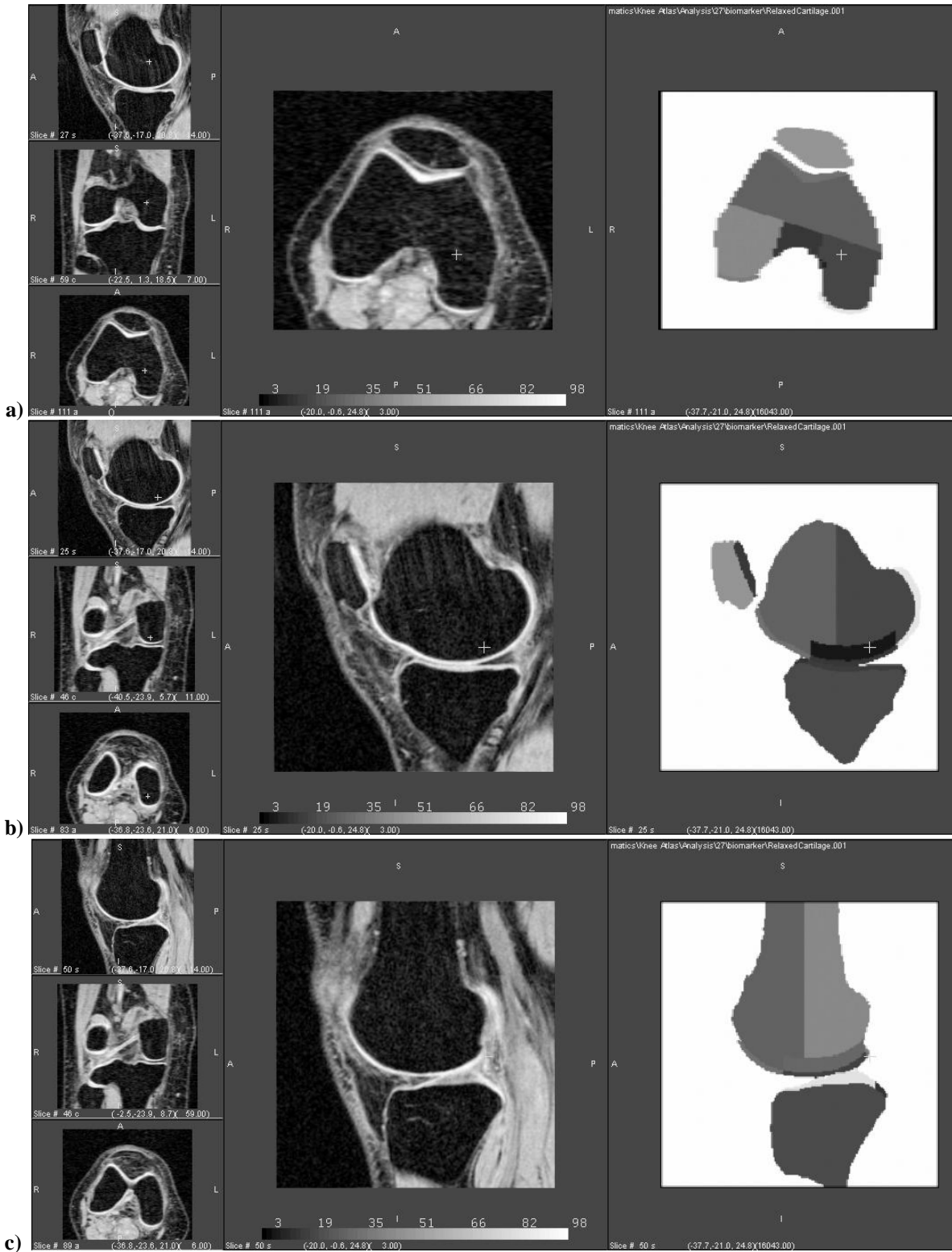


Figure 2: a) Axial cut of the femoral and cartilage regions. b) Medial slice of the knee and its corresponding classification. c) Lateral slice of the knee. The artificial weight bearing regions overlap the natural definitions of the posterior and the trochlea regions of the knee.

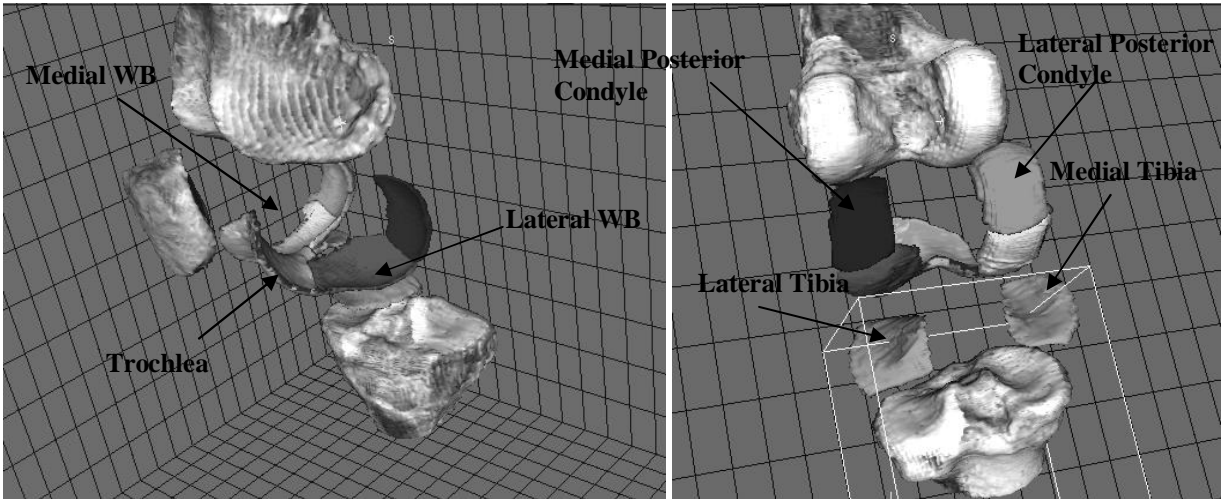


Figure 3: 3D reconstruction of the different femoral and tibia cartilage regions obtained by the proposed method: trochlea, medial weight bearing (WB) of the femur, lateral WB of the femur, medial posterior condyle, lateral posterior condyle, medial tibia and lateral tibia cartilages.

3. RESULTS

Once all the 18 segmentations were carried out, they were inspected by a musculoskeletal radiologist. Inspection demonstrated that the cartilage regions and the classification of the cartilage tissues into medial and lateral were always correct. Furthermore, the volume, thickness, and bone cartilage interface area were computed for the following cartilage regions: trochlea, medial weight bearing area of the femur, lateral weight bearing area of the femur, posterior aspect of the medial condyle, posterior aspect of the lateral condyle, tibia medial plateau and tibia lateral plateau. Once those metrics were extracted, the performance analysis was done by comparing the original and the mirrored analysis. The paired analysis yielded 9 paired data sets that were used to compute the reproducibility of the method to analysis-re-analysis variations. Figure 4 shows the Bland-Altman plot of the percentage of femoral coverage of the five areas. Table 1 shows the percentage of coverage and the reproducibility of the coverage. The algorithm reproducibility was better than 0.7% on the coverage. The maximum population variability was for the coverage of the trochlea. The trochlea averaged a 37% coverage with a 3% population variability among the nine sampled subjects. The same data was used to compute the performance of the segmentation algorithm for the different biomarkers (volume, thickness, and bone cartilage interface area) for all the extracted regions plus the total femoral cartilage. Analysis of the systems performance was done on the transformed scale for volume and surface area. The volume was transformed by a cubic root operation and the surface area by the square root. Those transformations removed the error dependency to structure size, making examination of performance easier. Figure 5 shows the Bland-Altman plots of the measured values; while Table 2 shows the summary numbers for the Volume, Thickness and Bone-cartilage contact area. The same table reports the performance as TCV (Coefficient of Variation of the Transformed measured metric) of the system.

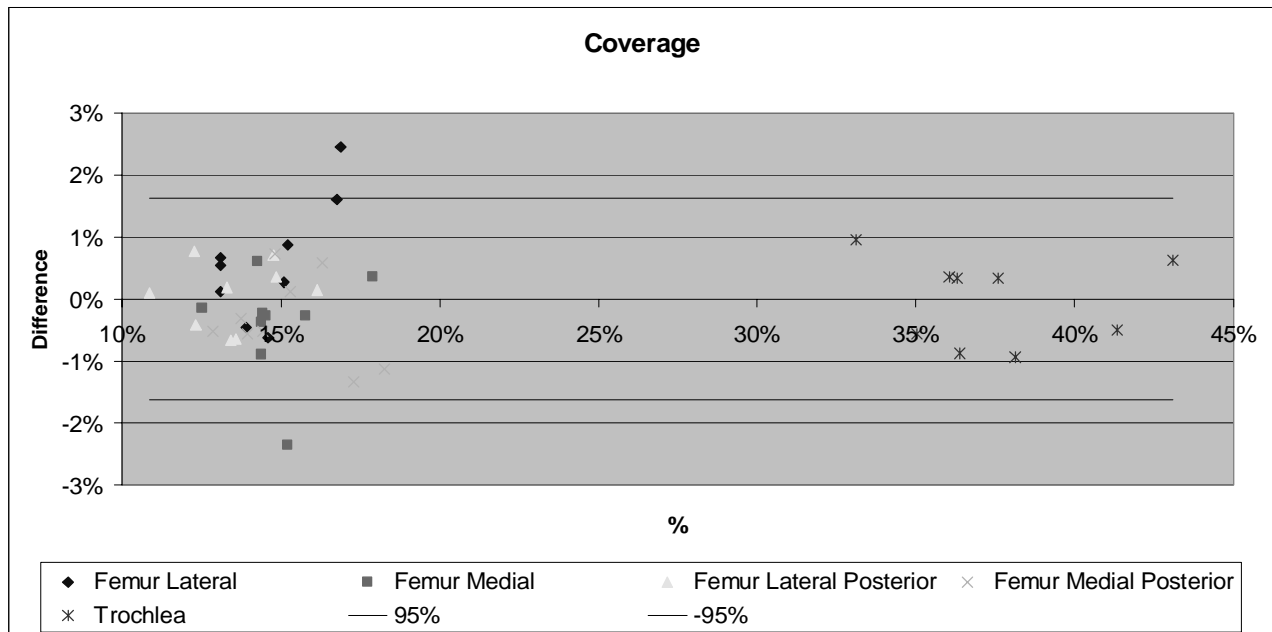


Figure 4: Bland-Altman Plot of the percentage of coverage of the analysis-re-analysis of the volunteer data sets.

Table 1: Area of coverage of the different femoral cartilage regions and the percentage of coverage from the whole total femur cartilage. The reproducibility of the coverage is small compared to the variability of percentage of coverage across the population.

		Weight Bearing		Posterior		Trochlea
		Medial	Lateral	Medial	Lateral	
Population	Average	710.60	701.51	727.95	650.57	1,814.47
	Stdev	121.00	126.75	118.40	147.78	413.18
	Reproducibility TCV	2.1%	1.7%	1.9%	1.4%	1.0%
Coverage	Average %	14.8%	14.6%	15.2%	13.5%	37.4%
	Stdev	1.5%	1.5%	1.8%	1.6%	3.1%
	Reproducibility RMS	0.6%	0.7%	0.5%	0.4%	0.5%

Table 2: Summary of the cartilage morphology and reproducibility of the cartilage regions for the 9 subjects. The performance of the cartilage regions is measured in the transformed scale from the randomized and blinded analysis-re-analysis data.

		Total	Weight Bearing		Posterior		Trochlea	Tibia		Pooled
		Femur	Medial	Lateral	Medial	Lateral		Medial	Lateral	Summary
Volume	Average	10,829.0	1,386.2	1,415.7	1,680.3	1,461.6	4,368.6	1,909.9	2,468.9	2,098.7
	Stdev	3,927.3	507.3	525.9	481.5	659.1	1,810.6	627.0	826.8	1,309.8
	Reproducibility TCV	0.9%	1.2%	1.4%	2.5%	1.3%	0.5%	1.5%	0.8%	1.5%
Contact Area	Average	4,818.6	710.6	701.5	728.0	650.6	1,814.5	1,010.1	983.5	942.7
	Stdev	876.1	121.0	126.8	118.4	147.8	413.2	168.7	179.4	430.1
	Reproducibility TCV	0.7%	2.1%	1.7%	1.9%	1.4%	1.0%	0.9%	0.9%	1.5%
Thickness	Average	2.04	1.78	1.86	2.02	1.91	2.27	1.79	2.41	2.01
	Stdev	0.39	0.36	0.43	0.32	0.41	0.51	0.35	0.52	0.46
	Reproducibility CV	1.8%	2.8%	1.7%	4.0%	2.7%	1.5%	3.0%	1.5%	2.5%

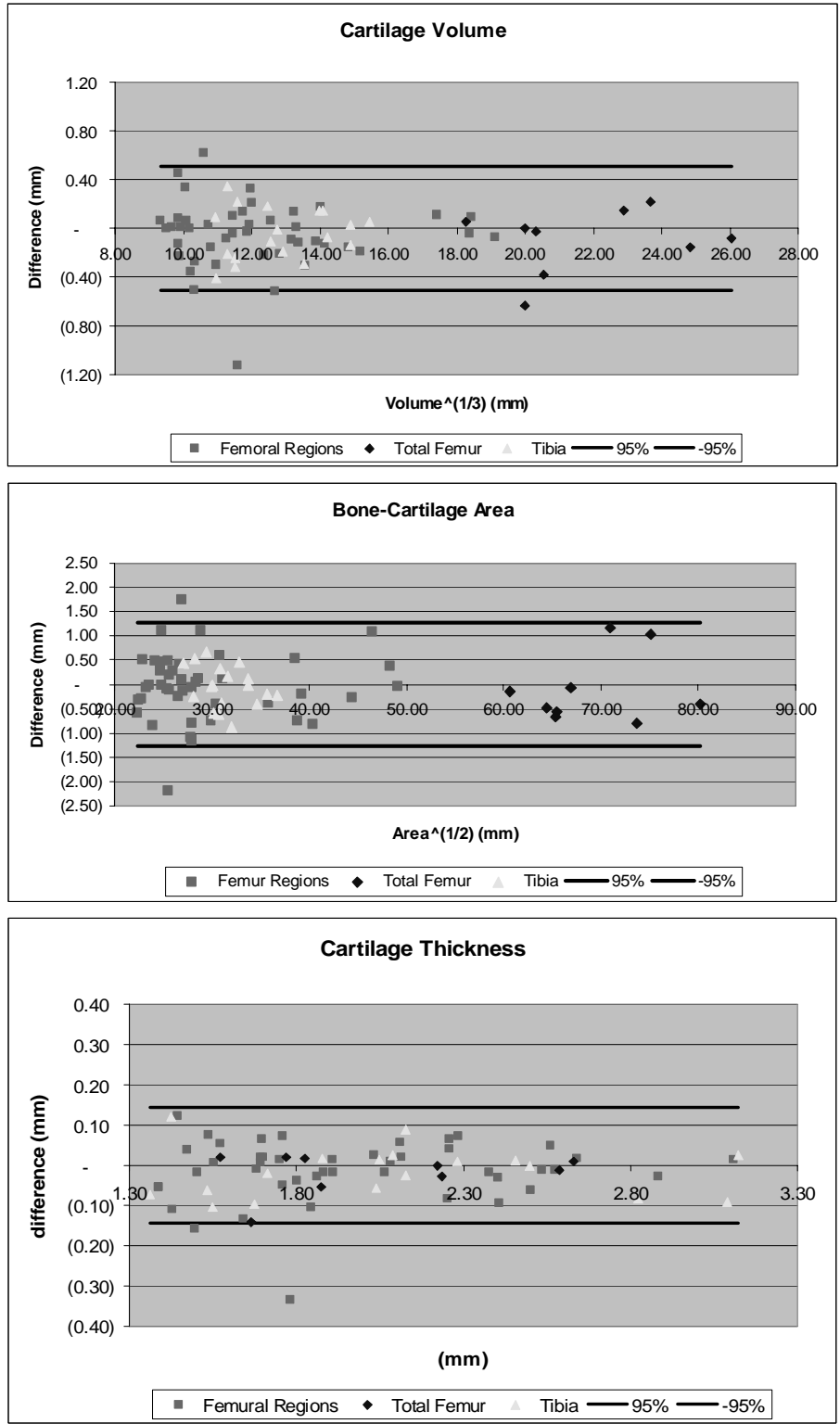


Figure 5: Bland-Altman plots of the transformed volume, the transformed contact area and the thickness measurements for the trochlea, medial and lateral weight bearing areas of the femur, the medial and lateral posterior condyles, and the medial and lateral tibia cartilage measurements. The variability of all measurements shows a nice performance of the measurements across the measured values.

4. CONCLUSIONS

We have presented an automated approach for subdividing the femoral cartilage into five different regions and the tibia cartilage into the medial and lateral regions. The division follows bone landmarks that can accurately be found by the computer algorithm, making the method highly reproducible. The application of the method on nine volunteers and simulated contra-lateral scans showed that the approach did not have any problem in identifying left knees from right knees. The amount of coverage among the nine different volunteers was very similar. The method provided reproducible measurements for volume, thickness and bone cartilage surface areas for all subdivided regions. This subdivision, did not impact seriously the reproducibility of this morphological parameters. The reproducibility of the five femoral was similar to the reproducibility of the tibia regions and the total femoral cartilage. This method improves the quantification of morphological cartilage parameters compared to subjective or supervised methods. This approach will help in the objective evaluation of the natural evolution of OA, and targeted OA therapies.

ACKNOWLEDGMENTS

The authors would like to thank Patricia C. Gonzalez, Therese Crilly, Bill Badger, Lisa Bamford, Ed Durkin and Larry Molinelli for their efforts related to this work. Financial support was provided by VirtualScopics, Inc.

REFERENCES

1. Felson DT, "An update on the pathogenesis and epidemiology of osteoarthritis", *Radiol. Clin. North Am*, **42**, 1-9, 2004.
2. Sarzi-Puttini P, Cimmino MA, Scarpa R, Caporali R, Parazzini F, Zaninelli A, Atzeni F, Canesi B, "Osteoarthritis: an overview of the disease and its treatment strategies", *Semin. Arthritis Rheum*, **35**, 1-10, 2005.
3. Beuf O, Ghosh S, Newitt DC, Link TM, Steinbach L, Ries M, Lane N, Majumdar S, "Magnetic resonance imaging of normal and osteoarthritic trabecular bone structure in the human knee", *Arthritis Rheum*, **46**, 385-393, 2002.
4. Felson DT, McLaughlin S, Goggins J, LaValley MP, Gale ME, Totterman S, Li W, Hill C, Gale D, "Bone marrow edema and its relation to progression of knee osteoarthritis", *Ann. Intern. Med*, **139**, 330-336, 2003.
5. Sowers MF, Hayes C, Jamadar D, Capul D, Lachance L, Jannausch M, Welch G, "Magnetic resonance-detected subchondral bone marrow and cartilage defect characteristics associated with pain and X-ray-defined knee osteoarthritis", *Osteoarthritis and Cartilage*, **11**, 387-393, 2003.
6. Blumenkrantz G, Lindsey CT, Dunn TC, Jin H, Ries MD, Link TM, Steinbach LS, Majumdar S, "A pilot, two-year longitudinal study of the interrelationship between trabecular bone and articular cartilage in the osteoarthritic knee", *Osteoarthritis and Cartilage*, **12**, 997-1005, 2004.
7. Conaghan PG, Felson DT, "Structural associations of osteoarthritis pain: lessons from magnetic resonance imaging", *Novartis. Found. Symp*, **260**, 191-201, discussion; 201-5, 277-9, 191-201, 2004.
8. Eckstein F, Glaser C, "Measuring cartilage morphology with quantitative magnetic resonance imaging", *Semin. Musculoskelet. Radiol*, **8**, 329-353, 2004.
9. Recht MP, Kramer J, Marcelis S, Pathria MN, Trudell D, Haghghi P, Sartoris DJ, Resnick D, "Abnormalities of articular cartilage in the knee: analysis of available MR techniques", *Radiology*, **187**, 473-478, 1993.
10. Disler DG, McCauley TR, Kelman CG, Fuchs MD, Ratner LM, Wirth CR, Hospodar PP, "Fat-suppressed three-dimensional spoiled gradient-echo MR imaging of hyaline cartilage defects in the knee: comparison with standard MR imaging and arthroscopy", *AJR Am. J Roentgenol*, **167**, 127-132, 1996.
11. Peterfy CG, Guermazi A, Zaim S, Tirman PF, Miaux Y, White D, Kothari M, Lu Y, Fye K, Zhao S, Genant HK, "Whole-Organ Magnetic Resonance Imaging Score (WORMS) of the knee in osteoarthritis", *Osteoarthritis and Cartilage*, **12**, 177-190, 2004.
12. Ding C, Garnero P, Cicuttini F, Scott F, Cooley H, Jones G, "Knee cartilage defects: association with early radiographic osteoarthritis, decreased cartilage volume, increased joint surface area and type II collagen breakdown", *Osteoarthritis and Cartilage*, **13**, 198-205, 2005.

13. Ding C, Cicuttini F, Scott F, Cooley H, Jones G, "Association between age and knee structural change: a cross sectional MRI based study", *Ann. Rheum. Dis*, **64**, 549-555, 2005.
14. Ding C, Cicuttini F, Scott F, Cooley H, Jones G, "Knee structural alteration and BMI: a cross-sectional study", *Obes. Res*, **13**, 350-361, 2005.
15. Bredella MA, Tirman PF, Peterfy CG, Zarlingo M, Feller JF, Bost FW, Belzer JP, Wischer TK, Genant HK, "Accuracy of T2-weighted fast spin-echo MR imaging with fat saturation in detecting cartilage defects in the knee: comparison with arthroscopy in 130 patients", *AJR Am. J. Roentgenol*, **172**, 1073-1080, 1999.
16. Felson DT, Chaisson CE, Hill CL, Totterman SM, Gale ME, Skinner KM, Kazis L, Gale DR, "The association of bone marrow lesions with pain in knee osteoarthritis", *Ann. Intern. Med*, **134**, 541-549, 2001.
17. Raynauld JP, Kauffmann C, Beaudoin G, Berthiaume MJ, de Guise JA, Bloch DA, Camacho F, Godbout B, Altman RD, Hochberg M, Meyer JM, Cline G, Pelletier JP, Martel-Pelletier J, "Reliability of a quantification imaging system using magnetic resonance images to measure cartilage thickness and volume in human normal and osteoarthritic knees", *Osteoarthritis and Cartilage*, **11**, 351-360, 2003.
18. Raynauld JP, Martel-Pelletier J, Berthiaume MJ, Labonte F, Beaudoin G, de Guise JA, Bloch DA, Choquette D, Haraoui B, Altman RD, Hochberg MC, Meyer JM, Cline GA, Pelletier JP, "Quantitative magnetic resonance imaging evaluation of knee osteoarthritis progression over two years and correlation with clinical symptoms and radiologic changes", *Arthritis Rheum*, **50**, 476-487, 2004.
19. Tamez-Pena JG, Barbu-McInnis M, Jackson R, Yu J, Eaton C, Totterman S, "Cartilage quantification: comparison between 3T DESS and 3T FLASH sequences", *Osteoarthritis and Cartilage*, 13 (Suppl. A): S124 [abstract]-, 2005.
20. Eckstein F, Hudelmaier M, Wirth W, Kiefer B, Jackson R, Yu J, Eaton C, Schneider E, "Double Echo Steady State (DESS) Magnetic Resonance Imaging of Knee Articular Cartilage at 3 Tesla - a Pilot Study for the Osteoarthritis Initiative", *Ann. Rheum. Dis*, 2005. (in press)
21. Burgkart R, Glaser C, Hyhlik-Durr A, Englmeier KH, Reiser M, Eckstein F, "Magnetic resonance imaging-based assessment of cartilage loss in severe osteoarthritis: accuracy, precision, and diagnostic value", *Arthritis Rheum*, **44**, 2072-2077, 2001.
22. Graichen H, Eisenhart-Rothe R, Vogl T, Englmeier KH, Eckstein F, "Quantitative assessment of cartilage status in osteoarthritis by quantitative magnetic resonance imaging: technical validation for use in analysis of cartilage volume and further morphologic parameters", *Arthritis Rheum*, **50**, 811-816, 2004.
23. Cohen ZA, McCarthy DM, Kwak SD, Legrand P, Fogarasi F, Ciaccio EJ, Ateshian GA, "Knee cartilage topography, thickness, and contact areas from MRI: in-vitro calibration and in-vivo measurements", *Osteoarthritis and Cartilage*, **7**, 95-109, 1999.
24. Hohe J, Ateshian G, Reiser M, Englmeier KH, Eckstein F, "Surface size, curvature analysis, and assessment of knee joint incongruity with MRI in vivo", *Magn Reson. Med*, **47**, 554-561, 2002.
25. Lee KY, Dunn TC, Steinbach LS, Ozhinsky E, Ries MD, Majumdar S, "Computer-aided quantification of focal cartilage lesions of osteoarthritic knee using MRI", *Magn Reson. Imaging*, **22**, 1105-1115, 2004.
26. Lee KY, Masi JN, Sell CA, Schier R, Link TM, Steinbach LS, Safran M, Ma B, Majumdar S, "Computer-aided quantification of focal cartilage lesions using MRI: accuracy and initial arthroscopic comparison" *Osteoarthritis and Cartilage*, **13**, 728-737, 2005.
27. Graichen H, Al Shamari D, Hinterwimmer S, Eisenhart-Rothe R, Vogl T, Eckstein F, "Accuracy of quantitative magnetic resonance imaging in the detection of ex vivo focal cartilage defects", *Ann. Rheum. Dis*, **64**, 1120-1125, 2005.
28. Hyhlik-Dürr A, Faber S, Burgkart R, Stammberger T, Maag KP, Englmeier KH, Reiser M, Eckstein F, "Precision of tibial cartilage morphometry with a coronal water-excitation MR sequence", *Eur. Radiol*, **10**, 297-303, 2000.
29. Glaser C, Burgkart R, Kutschera A, Englmeier KH, Reiser M, Eckstein F, "Femoro-tibial cartilage metrics from coronal MR image data: Technique, test-retest reproducibility, and findings in osteoarthritis", *Magn Reson. Med*, **50**, 1229-1236, 2003.
30. Eckstein F, Westhoff J, Sittek H, Maag KP, Haubner M, Faber S, Englmeier KH, Reiser M, "In vivo reproducibility of three-dimensional cartilage volume and thickness measurements with MR imaging", *AJR Am. J. Roentgenol*, **170**, 593-597, 1998.
31. Hunter D, Niu J, Zhang Q, McLennan C, LaValley M, Tu X, Hudelmaier M, Eckstein F, Felson D, "Cartilage volume must be normalized to bone surface area in order to provide satisfactory construct validity: The Framingham Study", *Osteoarthritis and Cartilage*, 12 [Suppl. B]: S2-, 2004.
32. Cicuttini F, Ding C, Wluka A, Davis S, Ebeling PR, Jones G, "Association of cartilage defects with loss of knee cartilage in healthy, middle-age adults: a prospective study", *Arthritis Rheum*, **52**, 2033-2039, 2005.

33. Phan CM, Link TM, Blumenkrantz G, Dunn TC, Ries MD, Steinbach LS, Majumdar S, "MR imaging findings in the follow-up of patients with different stages of knee osteoarthritis and the correlation with clinical symptoms", *Eur. Radiol*, 1-11, 2005.
34. Peterfy C, White D, Zhao J, VanDijke CF, Genant HK, "Longitudinal measurement of knee articular cartilage volume in osteoarthritis", *Arthritis Rheum*, 41 (Suppl. 9): S361 [abstract], 1998
35. Tamez-Pena J, Barbu-McInnis M, Totterman S, "Knee Cartilage Extraction and Bone-Cartilage Interface Analysis from 3D MRI Data Sets", *SPIE Medical Imaging*, **5370**, 1774-1784, 2004.
36. Tamez-Pena J, Barbu-McInnis M, Totterman S, "Virtual Performance Assessment of 3D Quantification Systems". *SPIE Medical Imaging*, **5749**, 508-516, 2005.
37. Tamez-Pena J, Lerner A, Yao J, Salo AD, Totterman S, "Evaluation of Distance Maps from Fast GRE MRI as a tool to Study the Knee Joint Space", *SPIE: Medical Imaging: Physiology and Function: Methods, Systems, and Applications*, **5031**, 551-562, 2003.